Single-Particle Tracking: Models of Directed Transport

Michael J. Saxton
Institute of Theoretical Dynamics, University of California, Davis, California 95616; and Laboratory of Chemical Biodynamics, Lawrence Berkeley Laboratory, University of California, Berkeley, California 94720 USA

ABSTRACT Single-particle tracking techniques make it possible to measure motion of individual particles on the cell surface. In these experiments, individual trajectories are observed, so the data analysis must take into account the randomness of individual random walks. Methods of data analysis are discussed for models combining diffusion and directed motion. In the uniform flow model, a tracer simultaneously diffuses and undergoes directed motion. In the conveyor belt model, a tracer binds and unbinds to a uniform conveyor belt moving with constant velocity. If a tracer is bound, it moves at the velocity of the conveyor belt; if it is unbound, it diffuses freely. Trajectories are analyzed using parameters that measure the extent and asymmetry of the trajectory. A method of assessing the usefulness of such parameters is presented, and pitfalls in data analysis are discussed. Joint probability distributions of pairs of extent and asymmetry parameters are obtained for a pure random walk. These distributions can be used to show that a trajectory is not likely to have resulted from a pure random walk.

INTRODUCTION

New techniques of single-particle tracking (Anderson et al., 1992; de Brabander et al., 1991; Edidin et al., 1991; Fein et al., 1993; Ghosh and Webb, 1987, 1994; Kucik et al., 1990; Kusumi et al., 1993; Lee et al., 1993; Sheetz et al., 1989) make it possible to measure lateral motion in cell membranes at a spatial resolution at least an order of magnitude higher than in fluorescence photobleaching recovery experiments. Furthermore, the number of diffusing particles averaged over is reduced from hundreds or thousands to one. In tracking experiments, proteins or lipids are labeled with colloidal gold microspheres or a highly fluorescent label, and computer-enhanced video microscopy is used to track the trajectories of individual particles as they move on the cell surface. This technique makes it possible to examine processes such as free diffusion, hindered diffusion, binding to immobile species, directed transport, trapping of particles in bounded microdomains, and transitions among these types of motion (Sheetz, 1993; Sheetz and Elson, 1993; Zhang et al., 1993).

Observation of the motion of individual particles increases the amount of information gained from an experiment enormously, but it also means that one must consider the randomness of a single random walk. As shown earlier (Saxton, 1993), trajectories suggesting directed transport or trapping in bounded microdomains frequently occur by chance in a pure random walk. To interpret observed trajectories, one must use the proper control, a two-dimensional unobstructed random walk. It is useful to define parameters to characterize the trajectories, such as measures of extent and measures of asymmetry. Then one can calculate the probability distributions of these parameters for directed motion and an unobstructed random walk, and use these probability distributions to test for directed motion. The overlap of the probability distributions shows that there are many ambiguous trajectories.

Experimental measurements of trajectories (see Qian et al., 1991; Ghosh and Webb, 1994) are limited by instrumental resolution, and more importantly by the total observation time before a particle goes out of focus, changes its mode of motion, or is internalized. Spatial resolution is high, ~5–50 nm. Temporal resolution is often set by the standard video rate of 30 frames/s, and the number of position measurements within the total observation time for a given particle may be low, between hundreds and thousands depending on the cell and the labeled species. The stochastic nature of a random walk is therefore important, and the number of time steps in the Monte Carlo calculations needs to be in the range of the number of experimental position measurements for a single particle.

We examine two models of directed transport. In the uniform flow model, a tracer simultaneously diffuses and undergoes directed motion. This model could be applied to cellular locomotion (Lee et al., 1993) and growth of nerve cells (Popov et al., 1993), as well as to the Bretscher bulk flow hypothesis (Sheetz, 1993). In the conveyor belt model, cytoskeletal elements are assumed to form a spatially uniform conveyor belt moving with a fixed velocity. If a tracer is bound to the conveyor belt, it moves at the velocity of the conveyor belt; if it is not bound, it diffuses freely. At each time step, the tracer tries to bind or unbind with the appropriate probabilities. Both models assume continuum diffusion, not lattice diffusion.

This paper extends previous work (Saxton, 1993) to a continuum model of directed transport. It shows a way to test the usefulness of a parameter in analyzing experimental data, and points out some pitfalls in data analysis. It shows how to use two-dimensional distributions of parameters to test whether a trajectory is likely to be a pure random walk. Parameters based on the radius of gyration tensor are used, but the aim of this paper is to show more generally how one can and cannot interpret parameters in single-particle tracking experiments.

Received for publication 17 June 1994 and in final form 28 August 1994.
Address reprint requests to Dr. Michael J. Saxton, Institute of Theoretical Dynamics, University of California, Davis, CA 95616-8618. Tel.: 916-752-6163; Fax: 916-752-7297; E-mail: mjsaxton@ucdavis.edu.
© 1994 by the Biophysical Society
0006-3495/94/11/2110/10 $2.00

METHODS

In the continuum diffusion model, a tracer is placed at a random initial position, and carries out a random walk of fixed step size in a system with periodic boundary conditions. The system size is 1×1, and the step size is 0.002915 (chosen for reasons involving obstructed diffusion in work to be published separately). The trajectory of the tracer is recorded and parameters characterizing the trajectory are calculated as described previously (Saxton, 1993). Typically, a random walk of 256 steps is carried out for 5×10^6 to 1×10^8 trajectories. The number of time steps is in the same range as a typical number of experimental observations of an individual particle. The large number of repetitions is needed to reduce statistical noise in the two-dimensional histograms; the one-dimensional histograms are therefore very reproducible.

To draw curves through the data points in some of the histograms, Catmull-Rom splines (Foley et al., 1990) are used. These interpolating splines provide smooth curves very much like what one would draw by hand.

RESULTS

The models

To examine directed transport, a continuum model is much more convenient than a lattice model. Furthermore, the probability distributions of parameters from a continuum model do not have spurious peaks resulting from the lattice structure. In the triangular lattice model, the random walk has a fixed step size of one lattice spacing, and the angles of the jumps are restricted to multiples of 60°. In the continuum model used here, the step size is still fixed, but the angle of the jump is unrestricted. An angle θ between 0 and 2π is chosen randomly, and the tracer is moved by

$$\Delta x = \ell \cos \theta, \tag{1a}$$

$$\Delta y = \ell \sin \theta, \tag{1b}$$

where ℓ is the step size. In a full continuum model, the angle of the jump would again be a random number uniformly distributed between 0 and 2π, but the step length would be a random variable chosen from a Gaussian distribution, because the jump is itself that random walk that occurs between consecutive observations.

In the uniform flow model, diffusion and directed transport are superimposed. At each time step, the tracer moves by the sum of a random step and a move in the x-direction by a constant amount. So

$$\Delta x = \ell \cos \theta + \tau V, \tag{2a}$$

$$\Delta y = \ell \sin \theta, \tag{2b}$$

where V is the velocity and τ is the jump time. The velocity is independent of position and time. The mean-square displacement is

$$\langle r^2 \rangle = 4Dt + V^2 t^2. \tag{2c}$$

This model (Qian et al., 1991; Kusumi et al., 1993) simulates diffusion in a membrane moving with velocity V.

In the conveyor belt model, mobile cytoskeletal elements are assumed to form a uniform, homogeneous conveyor belt that can bind the tracer. If the tracer is free, it makes a purely diffusional move

$$\Delta x = \ell \cos \theta, \tag{3a}$$

$$\Delta y = \ell \sin \theta. \tag{3b}$$

If it is bound, it makes a purely translational move in the x-direction

$$\Delta x = \tau V, \tag{3c}$$

$$\Delta y = 0. \tag{3d}$$

At each time step, the tracer attempts to bind or unbind. If the tracer is free, it attempts to bind with probability τP_{ON}; if it is bound, it attempts to unbind with probability τP_{OFF}. The average time bound is $\tau_{BD} = 1/P_{OFF}$; the average time unbound is $\tau_{FREE} = 1/P_{ON}$. The fraction of time bound is

$$F_{BD} = \tau_{BD}/(\tau_{BD} + \tau_{FREE}), \tag{4a}$$

and the mean-square displacement is

$$\langle r^2 \rangle = 4(1 - F_{BD})Dt + F_{BD}^2 V^2 t^2. \tag{4b}$$

In a more detailed model, the conveyor belts would be localized. The moves would still be given by Eq. 3, a–d. A bound particle would still attempt to detach at each move, but a free particle would attempt to attach only if it is in one of the belt regions. This model will not be considered here because there are too many unknowns.

What is the relation of these models to reality? In the cell, there may be a spatially nonuniform distribution of cytoskeletal elements producing directed motion with a distribution of velocities. A tracer can bind and unbind from these elements, and there may be a distribution of binding constants. To obtain tractable models, we average out various quantities. First, in all models we neglect the possible distribution of velocities and binding constants. Second, we carry out a spatial average, yielding a uniform distribution of cytoskeletal elements, but we keep the on-off equilibrium. This is the uniform conveyor belt model. Third, if we also average over time, the tracer is bound at all positions and all times, yielding the uniform flow model with $D = 0$. Here the tracer moves with an average velocity equal to the product of the velocity of the cytoskeletal element and the fraction of time bound. The uniform flow model with $D \neq 0$ is applicable to a cell in which the membrane is moving uniformly.

Units

To relate Monte Carlo results to experimental results, we use the following conversions. The unit of time τ is the time between observations of the tracer position, typically 1/30 s. The diffusion coefficient in an unobstructed system with no directed motion is D_0. These give the unit of length ℓ, defined by

$$\ell^2 = 4D_0\tau, \tag{5}$$

and the unit of velocity

$$V_0 = \ell/\tau. \tag{6}$$

The dimensionless Monte Carlo units D^*, r^*, t^*, and V^* are related to physical units D, r, t, and V by $D^* = D/D_0$, $r^* =$

r/ℓ, $t^* = t/\tau$, and $V^* = V/V_0$. It is assumed that no obstructions are present, so $D^* = 1$. For simplicity, in the rest of the paper we drop the asterisks from the Monte Carlo variables. Typical experimental values are given in Table 1 for macrophages and fish keratocytes. The motion of fish keratocytes is rapid (Kucik et al., 1990; Lee et al., 1993).

In analyzing experimental data, it may be useful to compile histograms of the velocity (Qian et al., 1991) or the step size. These distributions provide a way to distinguish diffusive motion from directed motion, and the mean step size for diffusive motion ℓ_{OBS} can be used to define D_0 from Eq. 5. This is similar to the procedure of Kusumi et al. (1993), who use the short-time diffusion coefficient as a normalization factor.

The problem

The problem we consider is how to detect directed motion in the presence of random motion. In principle, the solution is trivial. The mean-square displacement is $\langle r^2 \rangle \propto Dt$ for diffusion, and $\langle r^2 \rangle \propto V^2t^2$ for directed motion. So if the measurement is long enough and averaged over enough particles, the difference is obvious. (Qian et al. (1991) analyze in detail how the statistical errors in D and V vary with the duration of the measurement.) But in practice the number of particles may be small, and the observation time may be limited because the particles move out of focus or change their mode of motion.

Some trajectories for the uniform flow model are shown in Fig. 1, *a–c* for 256 time steps. Fig. 1 *a*, for $V = 0$, suggests pure diffusion, but several trajectories suggest directed motion in roughly the same direction, and several particles appear to be trapped. Fig. 1 *b*, for $V = 0.05$, suggests some directed motion, but one particle makes a U-turn, and several particles appear to be trapped. In Fig. 1 *c*, for $V = 0.10$, the directed motion is obvious, but one particle makes a U-turn, two appear to be trapped, and another appears to change from trapped to directed motion.

Fig. 1, *d–f* shows trajectories for three specific examples of the conveyor belt model. Fig. 1 *d* shows trajectories for mostly directed motion. Here $P_{ON} = 0.3125$ and $P_{OFF} = 0.034722$, so $\tau_{ON} = 28.8$ and $\tau_{OFF} = 3.2$. On the average there is an on-off cycle of 32 time steps with the tracer bound 90% of the time and freely diffusing 10% of the time. In a typical run time of 256 time steps, a tracer goes through an average of eight on-off cycles, though in fact the on-off cycle is not deterministic, and the tracer tries to change its binding at every time step. Fig. 1 *e* shows trajectories for an equal mixture of directed motion and diffusion. Here $P_{ON} = P_{OFF} = 0.0625$, so that a tracer is bound 50% of the time, with the same average on-off cycle of 32 steps. Fig. 1 *f* shows trajectories for the mostly diffusive case. Here $P_{ON} = 0.034722$ and $P_{OFF} = 0.3125$, so that a tracer is bound 10% of the time and freely diffusing 90% of the time, with the same average cycle time. These three examples do not go to the same limit as $V \rightarrow 0$. When V is 0, the tracer is immobilized a fraction F_{BD} of the time, so the effective diffusion coefficient is $D^* = 1 - F_{BD}$. In the same limit for the uniform flow model, $D^* \rightarrow 1$.

TABLE 1 Observed velocities

Parameters	Macrophages (Sheetz et al., 1989)	Fish keratocytes (Kucik et al., 1990)
V (nm/s)	20	350
D_0 (cm^2/s)	3.0×10^{-11}	3.5×10^{-10}
ℓ (nm)	20	68
V_0 (nm/s)	600	2000
V^*	0.03	0.17

The ambiguities remain in the next stage of data analysis, plots of the displacement r^2 as a function of time. Plots for three individual trajectories are shown in Fig. 2 *a*, again for $V = 0.0$, 0.05, and 0.10. One might be tempted to interpret the bottom curve as a period of trapping followed by a period of free diffusion; in fact it is pure diffusion. Or one might assume pure directed motion, fit all of these to parabolas, and extract the velocities. In fact, these are from the uniform flow model. At $t = 256$, the upper curve is for $V = 0.05$, and the curve just below it is for $V = 0.10$. If we average over a large number of trajectories, however, the fluctuations average out, yielding the expected curves in the expected order, as shown in Fig. 2 *b*. A similar plot for the conveyor belt model with 10% directed motion and 90% diffusion, averaged over many trajectories, shows little change in $\langle r^2 \rangle$ with V. This result suggests that, in the presence of experimental noise, much longer measurements will be needed to see a small component of directed motion in the presence of diffusion.

The results in Figs. 1 and 2 show the dangers of interpreting individual trajectories purely by eye. These results are not carefully selected examples of anomalies, but arbitrary random walks. Even though it is trivial to see differences in $\langle r^2 \rangle$, it is not necessarily trivial to see differences in r^2 for a single trajectory.

A solution

To solve this problem, we define parameters characterizing a trajectory, evaluate them by Monte Carlo calculations, and examine their probability distributions (Saxton, 1993). We can then compare observed trajectories with the proper control, an unobstructed pure two-dimensional random walk.

For a trajectory of n steps, the two-dimensional radius of gyration tensor ($\mathbf{T}$) is (Šolc and Stockmayer, 1971; Rudnick and Gaspari, 1987)

$$\mathbf{T} = \begin{pmatrix} \langle x^2 \rangle - \langle x \rangle^2 & \langle xy \rangle - \langle x \rangle \langle y \rangle \\ \langle xy \rangle - \langle x \rangle \langle y \rangle & \langle y^2 \rangle - \langle y \rangle^2 \end{pmatrix}, \quad (7)$$

where the averages are over all n steps in the trajectory: $\langle x \rangle = (1/n) \sum_{i=1}^{n} x_i$, and so forth. A different type of averaging is often used in analyzing experimental data (Qian et al., 1991; Ghosh, 1991). There, averaging is done within each trajectory, so that, e.g., the mean-square displacement for $t = 2$ is taken to be the average over all displacements (Qian et al., 1991), or all independent displacements (Ghosh, 1991), two time steps apart.

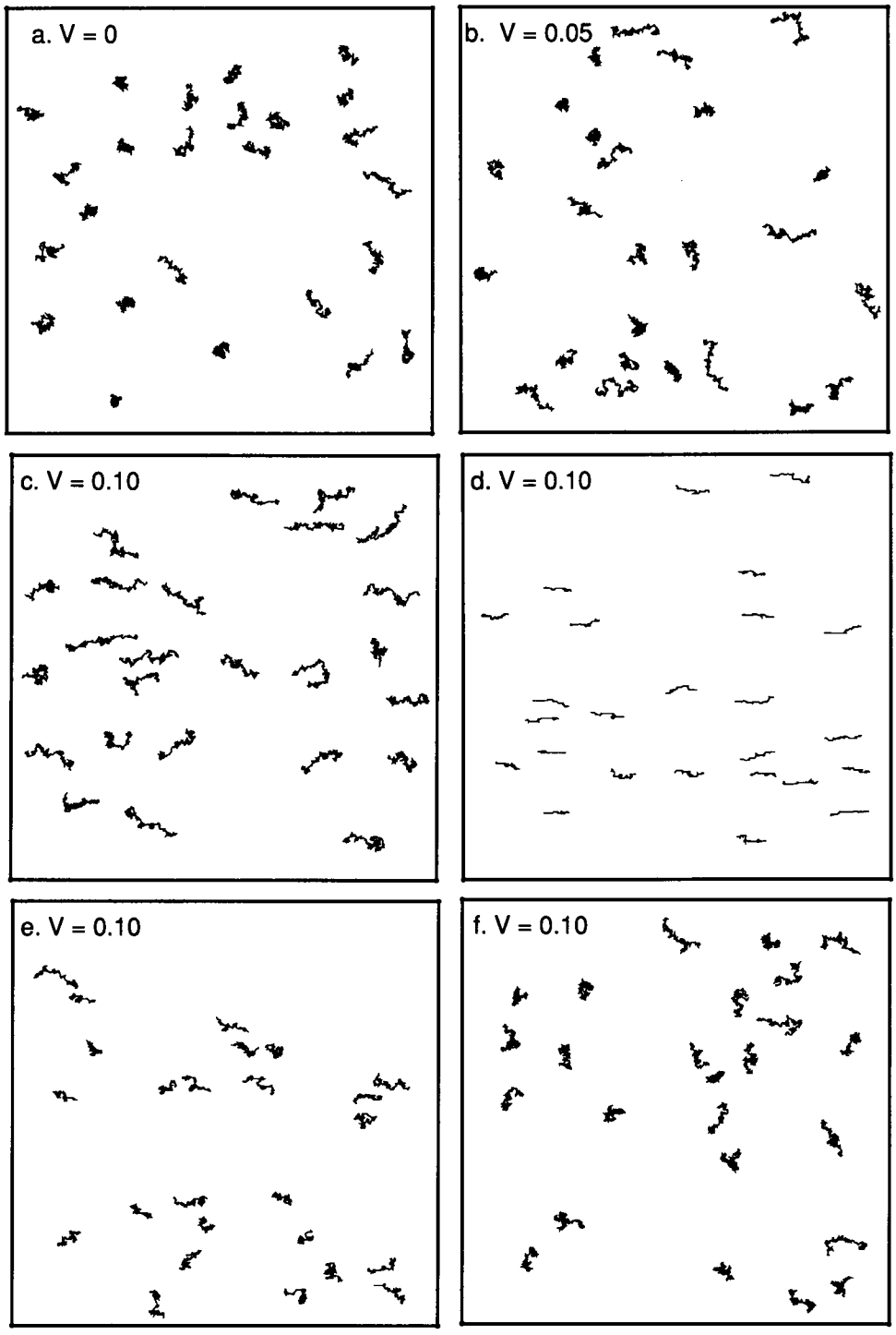

FIGURE 1 Trajectories for 25 particles and 256 time steps. Directed motion is horizontal in all cases. (*a–c*) Uniform flow model, for velocities $V = 0, 0.05$, and 0.10. (*d–f*) Conveyor belt model for $V = 0.10$. (*d*) 90% directed motion, 10% diffusion. (*e*) 50% directed motion, 50% diffusion. (*f*) 10% directed motion, 90% diffusion. Corresponding values of P_{ON} and P_{OFF} are given in the text.

The principal radii of gyration are the eigenvalues of the tensor **T**,

$$R_1^2, R_2^2 = \tfrac{1}{2}[(T_{xx} + T_{yy}) \pm \sqrt{(T_{xx} - T_{yy})^2 + 4T_{xy}^2}]. \quad (8)$$

To measure the extent of the trajectory, one can use the square displacement r^2, the square of the maximum distance R^2 from the initial point, or the radius of gyration

$$R_G^2 = R_1^2 + R_2^2. \quad (9)$$

To remove the time dependence due to diffusion, all of these are divided by time. For the models of directed motion treated here, there is no qualitative difference among the three measures of extent (except that R_G^2 is almost a factor of 10 smaller than the other two), so for simplicity r^2 will be used in most cases.

To measure the asymmetry of the trajectory, one can use the eigenvalue ratio, the ratio of the smaller to the larger principal radius of gyration (Family et al., 1985)

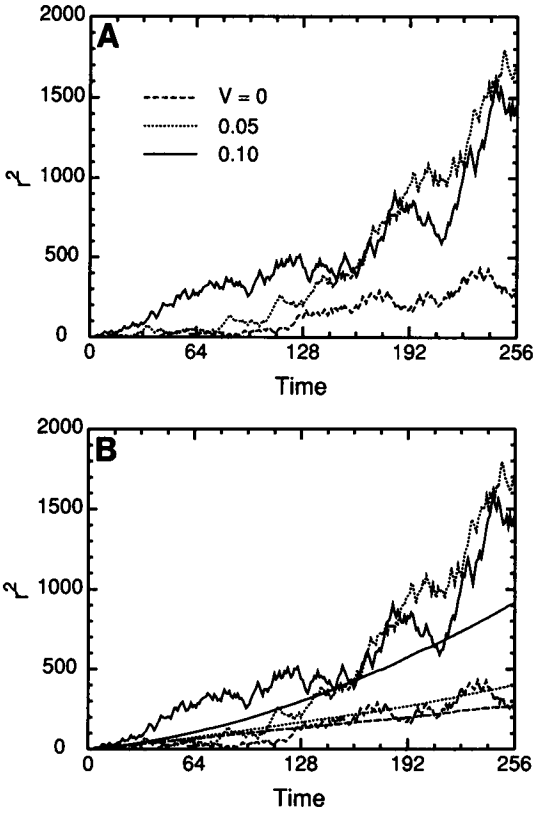

FIGURE 2 (*a*) Displacement r^2 as a function of time for three individual random walks in the uniform flow model, for the indicated velocities. (*b*) Mean-square displacement (r^2) as a function of time for the same velocities, superimposed on the displacements of Fig. 2 *a*. To obtain the mean-square displacements, the runs in (*a*) were continued and averaged over 1000 tracers.

$$a_2 = R_2^2/R_1^2. \tag{10}$$

Linear trajectories have $a_2 = 0$; circularly symmetric trajectories have $a_2 = 1$. Or one can use the asymmetry parameter

$$A_2 = \frac{(R_1^2 - R_2^2)^2}{(R_1^2 + R_2^2)^2}, \tag{11}$$

which is the deviation from circularity, normalized by the radius of gyration. This parameter is equal to 0 for circularly symmetric trajectories and 1 for linear trajectories (Quandt and Young, 1987; Rudnick and Gaspari, 1987).

Single-parameter distributions

For a given difference in V, the overlap of the histograms of a parameter indicates the effectiveness of that parameter in measuring V. Fig. 3 *a* shows the distribution of the eigenvalue ratio a_2 for the uniform flow model for $V = 0$ and 0.1, and $t = 256$. When $V = 0$, the histogram is peaked toward low eigenvalue ratios, because most random walks are asymmetric. When $V = 0.1$, the distribution shifts strongly toward even lower values of a_2, as expected, but the overlap of the curves is considerable. For the experimentalist, what this

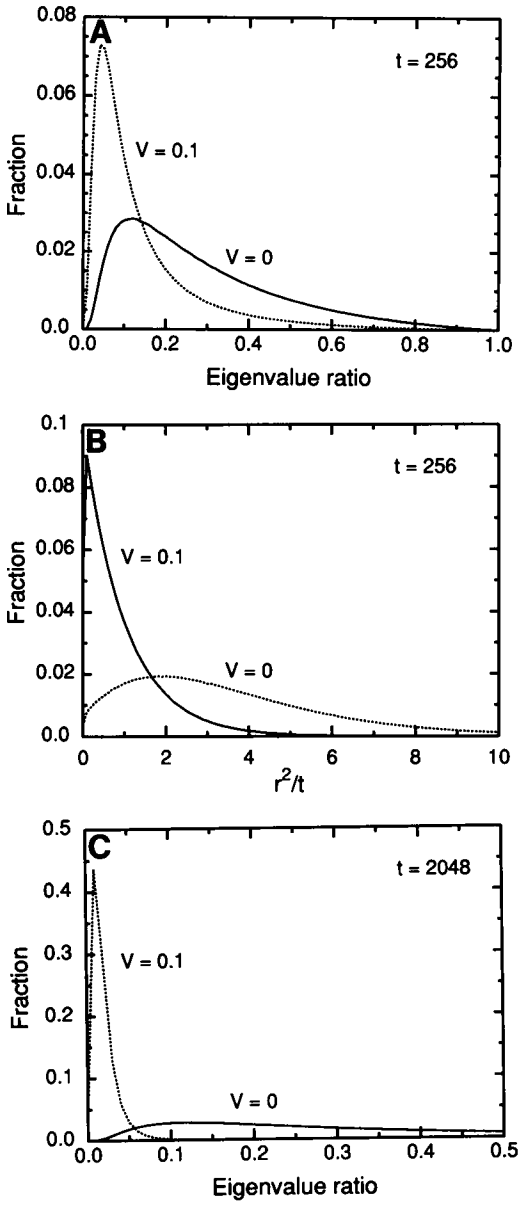

FIGURE 3 Distribution of parameters for the uniform flow model for $V = 0.0$ and 0.1. (*a*) Eigenvalue ratio a_2 for $t = 256$. (*b*) r^2/t for $t = 256$. (*c*) Eigenvalue ratio a_2 for $t = 2048$. The change between *a* and *c* is in the histogram for $V = 0.1$. For t this large, the histogram for $V = 0$ is independent of time. (Note the changes in scale.)

overlap implies is that many trajectories with $V = 0.1$ cannot be distinguished from purely diffusive trajectories using this parameter and this observation time. Furthermore, suppose that an experiment yields a mixture of apparently diffusive and apparently nondiffusive trajectories. The mixture might result from the presence of two populations of tracers with different dynamics, or from the distribution of trajectories within a single population of tracers.

How can the problem of overlap be solved? First, one can use a better parameter. Fig. 3 *b* shows histograms of r^2/t for the same conditions as Fig. 3 *a*. The overlap is less, and a significant fraction of the trajectories can be distinguished.

Second, one can use longer measurements, as shown in Fig. 3 *c*. Here most of the trajectories can be distinguished using the eigenvalue ratio; practically all can be distinguished using r^2/t. Third, one can observe multiple particles. A single particle may show anomalous behavior by chance, but if several particles show the same anomalous behavior, the probability is much lower. See, for example, Fig. 7 of Ghosh and Webb (1994).

For a given experiment, some parameters are better than others, but the problem of overlap will always occur. Whatever the parameter, it has some probability distribution, and for V small enough, this distribution will overlap the distribution for $V = 0$ significantly. Similarly, for trapping within a region of radius R, there will be overlap of the distributions as R decreases from infinity to 0.

Analysis as in Fig. 3 is useful for testing parameters, but for interpreting experimental data, these plots answer the wrong question. The question they answer is, if it is known that a trajectory results from either $V = 0$ or $V = 0.1$, how well can we distinguish between these alternatives using a given parameter and observation time? In reality, V is an unknown continuous variable, and we want to see how effectively a parameter measures V. It is necessary to carry the analysis one step further.

Velocity distributions

Given an observed parameter value, what distribution of velocities is consistent with it? For a particular model, we can obtain this distribution as follows. First, we generate histograms of the parameter for many values of V, as shown in Fig. 4 *a* for r^2/t. Then we pool this data into a two-dimensional histogram, shown as a contour map in Fig. 4 *b*. Finally, we slice this two-dimensional histogram in the other direction, and read off histograms of V at constant r^2/t, as shown in Fig. 4 *c*. These curves give the distribution of V consistent with an observed value of r^2/t. Each curve in Fig. 4 *c* is normalized to unit area because it is a conditional probability, the probability of a particular value of V given that r^2/t is observed to have a particular value. The overlap of the V curves indicates the usefulness of the parameter in measuring V.

Similar distributions of V for fixed values of r^2/t are shown in Fig. 5 *a* for the conveyor belt model for 90% directed motion, 10% diffusion, and in Fig. 5 *b* for 50% directed motion, 50% diffusion. As the fraction of time bound decreases, the peaks broaden considerably and the overlaps increase. For 10% directed motion, 90% diffusion, the V dependence is so weak that there is little reason to show the results. Fig. 5 *c* shows the distribution of V for fixed values of the asymmetry parameter A_2 for the uniform flow model. The eigenvalue ratio a_2 shows even less V dependence for these models of directed motion. These parameters are less useful than r^2/t in determining the velocity.

For the uniform flow model, diffusion and directed motion occur simultaneously, and the V curves are trivial to understand. The mean velocity is just V. For pure directed motion,

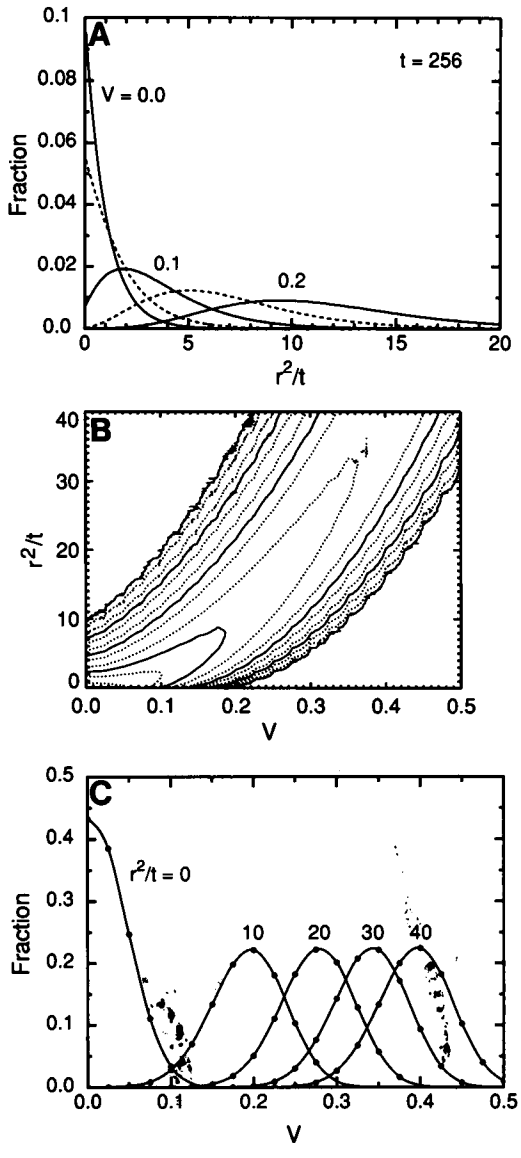

FIGURE 4 Construction of distributions of V for observed values of r^2/t. (*a*) Histograms of r^2/t for $V = 0, 0.05, 0.10, 0.15$, and 0.20 from Monte Carlo calculations for the uniform flow model at $t = 256$. For clarity, curves are shown at a spacing of $\Delta V = 0.05$ and a maximum of $V = 0.2$; in practice, a spacing of 0.025 and a maximum of 0.5–0.7 are used. (Kusumi et al. (1993) show similar families of curves for their relative deviation parameter *RD*. This parameter is similar to r^2/t, but differently averaged, and normalized by the short-time diffusion coefficient.) (*b*) Contour plot of the pooled data. The contours are 0.0001, 0.0002, 0.0005, . . . , 0.5; the solid lines correspond to powers of 10. (*c*) Distribution of V for the indicated values of r^2/t, obtained by slicing the data in Fig. 4 *b* parallel to the V-axis, and normalizing the resulting histograms. The points are Monte Carlo data and the curves are splines drawn through the data points.

$r = Vt$, and for pure diffusion, $\langle r^2 \rangle = Dt$ in dimensionless units, so the width of the curves is just $V = \sqrt{D/t}$, obtained by requiring that pure directed motion and pure diffusion yield the same values of $\langle r^2 \rangle / t$. The Monte Carlo curves are very close to these values. For the conveyor belt model, we can approximate the values similarly. The mean velocity (not the peak) is $F_{BD}V$. In dimensionless units, for directed motion

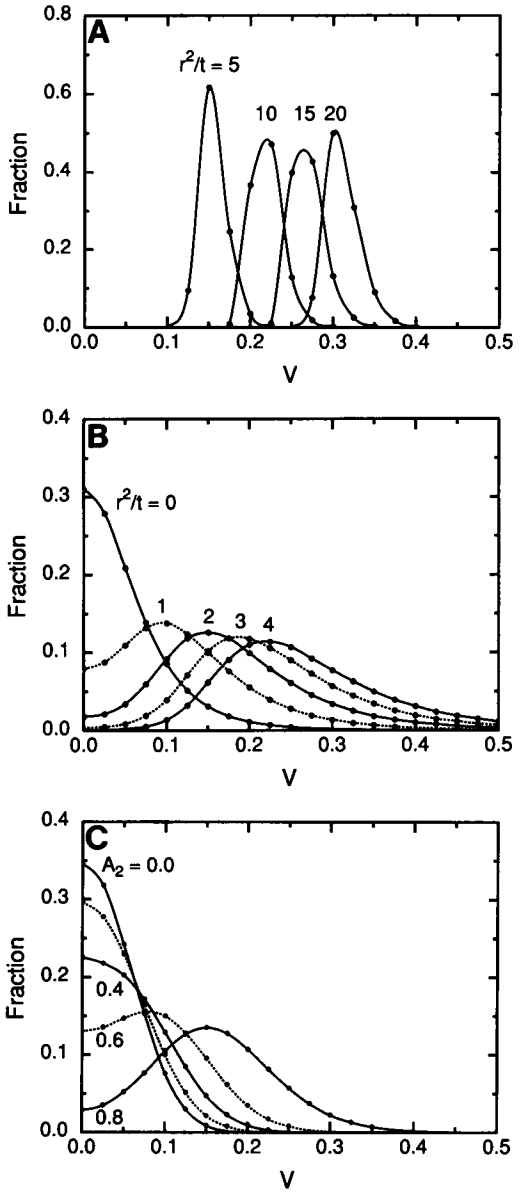

FIGURE 5 Distributions of V for observed values of parameters. (*a*) Distribution of V for the indicated values of r^2/t for the conveyor belt model with 90% directed motion, 10% diffusion. (*b*) The same distribution for the conveyor belt model with 50% directed motion, 50% diffusion (*c*). The distribution of V for A_2 = 0.0, 0.2, 0.4, 0.6, and 0.8 for the uniform flow model.

$r = F_{BD}Vt$, and for pure diffusion $\langle r^2 \rangle = (1 - F_{BD})Dt$, so the width of the curves is $V = \sqrt{(1 - F_{BD})D/F_{BD}^2 t}$. The mean velocities for the Monte Carlo curves are near these approximate values, but the Monte Carlo curves are wider than the estimates, because the estimate includes only broadening due to diffusion, and there is additional broadening due to fluctuations in the fraction of time the particle is diffusing.

Two-parameter plots

Another way to use these parameters is to look at two of them simultaneously. The obvious choice is an extent parameter and an asymmetry parameter. We consider the joint distribution of r^2/t and a_2 and the joint distribution of R_G^2/t and A_2 for the pure unobstructed random walk. From these distributions one can find the probability that an observed trajectory could have occurred in a pure random walk. A similar approach was used by Kusumi et al. (1993) to classify trajectories based on a single parameter. Fig. 6 *a* shows a contour plot of the joint distribution of r^2/t and a_2, and Fig. 6 *b* shows the joint distribution of R_G^2/t and A_2. The contours fall off very steeply at small values of r^2/t, a_2, and R_G^2/t. To give greater detail in these regions, the histograms were also collected using logarithmic bins. Fig. 6 *c* shows the joint distribution of r^2/t and a_2, with both variables in logarithmic bins, and Fig. 6 *d* shows the joint distribution of R_G^2/t and A_2, with R_G^2/t in logarithmic bins and A_2 in linear bins.

The qualitative behavior of the joint distribution is shown in Fig. 7 for pure diffusion, trapping, and both models of directed motion. As the velocity or the fraction of time spent in directed motion increases, the distribution moves toward lower a_2 and higher r^2/t. There is significant overlap of the distributions for pure diffusion (Fig. 7 *a*), trapping (Fig. 7 *b*), and 50% diffusion, 50% directed motion (Fig. 7 *d*).

The data used to generate Fig. 6, and a Fortran program to calculate the probability of a pair of experimental parameters from this data, is available from *Biophysical Journal* by FTP, or from the author by E-mail. This program simply takes the pair of experimental parameters, calculates the histogram indices as in the original Monte Carlo program, and looks up the size of the bin and the probability that a pure random walk lies within that bin. The distribution is normalized so that the probability of the most probable bin is 1. For example, if an experimental trajectory gave $r^2/t = 7$ and $a_2 = 0.2$, the linear bins (Fig. 6 *a*) give a probability of 7.2×10^{-5} that, for a pure random walk, the parameters are in the range 7.00, 7.25, and 0.20, 0.21 respectively. The logarithmic bins (Fig. 6 *c*) give a probability of 8.2×10^{-4} that, for a pure random walk, the parameters are in the range 6.3096, 7.9433, and 0.1995, 0.2512.

There is an important distinction to keep in mind when using this sort of data analysis. If the observed parameter falls on the fringes of the histogram for a pure random walk, one can legitimately say that the observed trajectory is not likely to be a pure random walk. But if the parameter falls near the center of the histogram for a pure random walk, one cannot say that the trajectory is likely to be a pure random walk. The trajectory could result from directed motion with a velocity for which the histograms overlap, as in Figs. 3 and 7, or from other mechanisms. Such trajectories cannot be classified as purely diffusive; they must be classified as "diffusive plus ambiguous."

Continuum versus lattice models

Finally, we compare results for the lattice and continuum simulations of unobstructed diffusion. The histogram of r^2/t is noisier for lattice simulations than for continuum simulations, as shown in Fig. 8. The calculations are done for 10^8

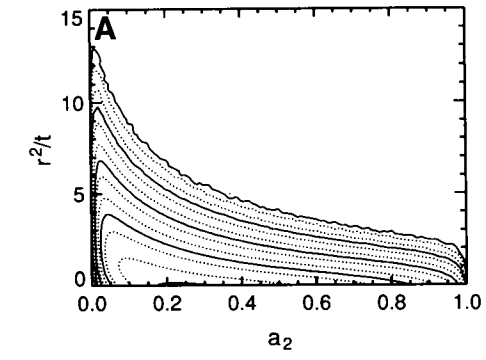

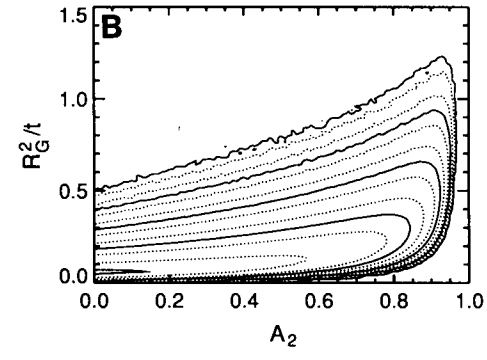

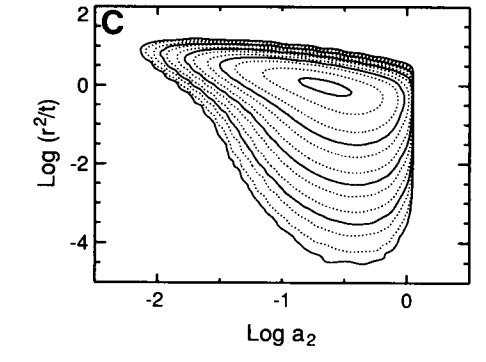

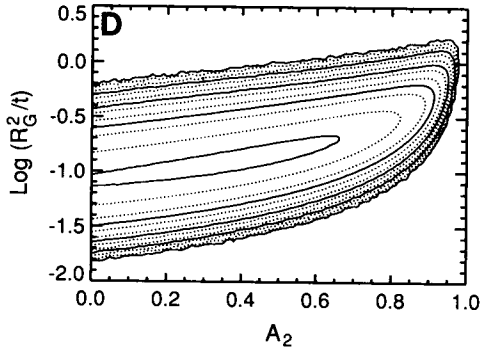

FIGURE 6 Joint distributions of extent and asymmetry parameters for a pure unobstructed random walk. Here $t = 256$, and 10^8 trajectories were used to get smooth contours at low probabilities. The distributions are normalized so that the maximum value is 1. Contours are 0.0001, 0.0002, 0.0005, . . . , 0.5, with the solid contours corresponding to powers of 10. The peak is indicated by a solid contour at 0.9. Linear bin sizes are 0.25 for r^2/t, 0.02 for R_G^2/t, and 0.01 for a_2 and A_2. Logarithmic bin sizes are 0.1 for all variables. (*a*) Joint distribution of r^2/t and a_2 with linear bins. (*b*) Joint distribution of R_G^2/t and A_2 with linear bins. (*c*) Joint distribution of r^2/t and a_2 with logarithmic bins. (*d*) Joint distribution of R_G^2/t and A_2 with logarithmic bins for R_G^2/t and linear bins for A_2.

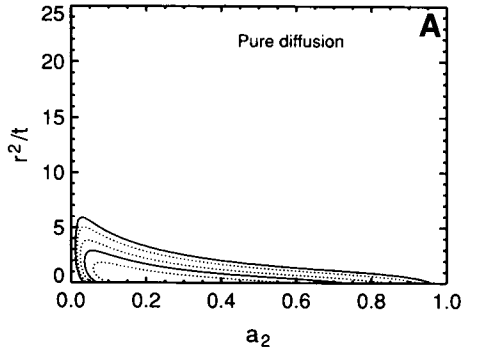

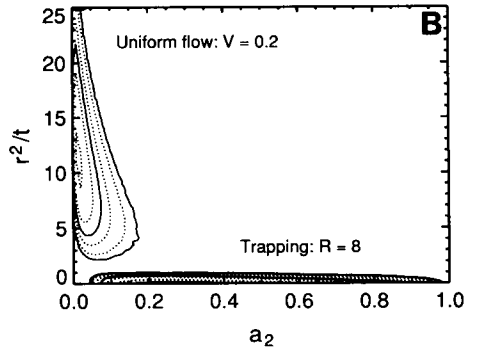

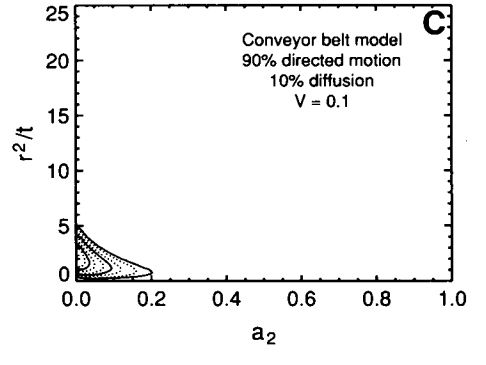

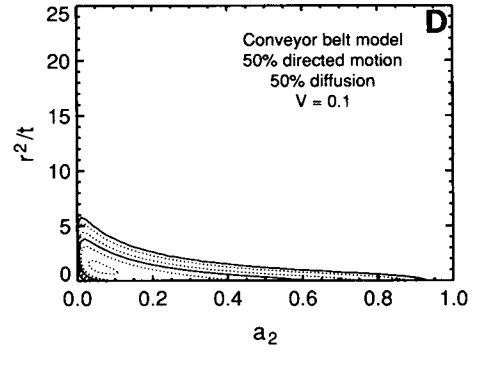

FIGURE 7 Joint distributions of r^2/t and a_2 with linear bins for pure diffusion, trapping, the uniform flow model, and the conveyor belt model. The distributions are normalized so that the total volume is one and the plots are directly comparable. Contour intervals are 0.0001, 0.0002, 0.0005, . . . , 0.05, with the solid lines corresponding to powers of 10. Only Fig. 7 *c* goes above 0.005. Bin sizes are 0.25 for r^2/t and 0.01 for a_2. (*a*) Pure diffusion. (*b*) Uniform flow model with $V = 0.2$. Trapping in a circular domain of radius 8 ℓ. (*c*) Conveyor belt model with 90% directed motion, 10% diffusion, and $V = 0.1$. (*d*) Conveyor belt model with 50% directed motion, 50% diffusion, and $V = 0.1$.

trajectories, so that the noise in the lattice simulation is a result of the lattice structure, not statistical noise. The histogram for R^2/t is similar to Fig. 8, but for R_G^2/t, A_2, and a_2, the histograms for lattice and continuum models agree closely. Fig. 9 *a* shows the joint distribution of r^2/t and a_2. Continuum and lattice diffusion give very similar results. Fig. 9 *b* shows the same joint distribution for the continuum model for $t = 64$ and $t = 256$. The contours are similar because a_2 approaches its asymptotic value quickly, and division by t removes the time dependence of r^2. The only major differences among contours in Fig. 9 are for the most extended trajectories, which have small eigenvalue ratios, large values of r^2/t, and low probabilities. Similar plots for the joint distribution of R_G^2 and A_2 show similarly close agreement for both linear and logarithmic bins. Agreement is poor for the contour plots with logarithmic bins of r^2/t, because the logarithmic bins emphasize small distances for which the lattice structure is important. Here it is necessary to use a continuum model.

DISCUSSION

The basic idea of this paper is that to analyze a trajectory, one must define a parameter characterizing the trajectory, and look at the probability distribution of that parameter for a pure random walk and for whatever models one thinks appropriate. The overlap of the probability distributions shows how well the measurement distinguishes the models. If the overlap is significant, several approaches may be useful: use better parameters, make longer measurements, or look for similar behavior of many particles. Or one might simply concede that many trajectories will be ambiguous and focus attention on the extreme trajectories. Earlier work (Saxton, 1993) emphasized the measures of asymmetry a_2 and A_2, but the results here (Fig. 3) indicate that r^2/t is a more useful parameter in testing for directed motion when a particle undergoes both diffusion and directed motion.

Trajectories can be analyzed using joint probability distributions of pairs of parameters characterizing the trajectories. The main application of these distributions is likely to be to show that an observed trajectory is not likely to have resulted from a random walk. In this paper the pairs of parameters have been chosen to be measures of extent and measures of asymmetry, but other choices are possible. (These two-dimensional histograms also show the degree of correlation or anticorrelation of the pair of parameters. Ideally, one would use two completely uncorrelated parameters.)

A comparison of probability distributions for lattice and continuum models of pure diffusion, with velocity 0 and no obstructions, showed surprisingly good agreement except for the most extended trajectories. This result supports the use of lattice simulations, which have the advantages of simplicity, speed, and the ability to examine the number of distinct sites visited. But in most cases, continuum simulations are preferable to reduce the noise in some of the probability distributions and to obtain results valid at small distances. For models including directed motion, continuum simulations are much more practical than lattice simulations.

An experimentalist observing a "conveyor belt" cell would like to be able to look at a trajectory and read off bound and free periods, the velocity during the bound periods, and the diffusion coefficient during the free periods. This is not yet possible. It would be useful to be able to subdivide a trajectory into bound and free periods, but doing this by eye is

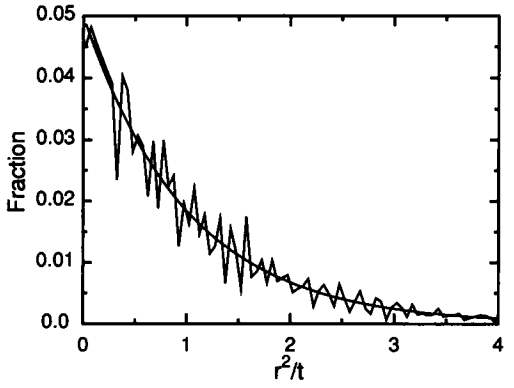

FIGURE 8 Distribution of displacement r^2/t for a pure random walk on a lattice (jagged line) and on a continuum (smooth line), for $t = 256$, and 10^8 trajectories.

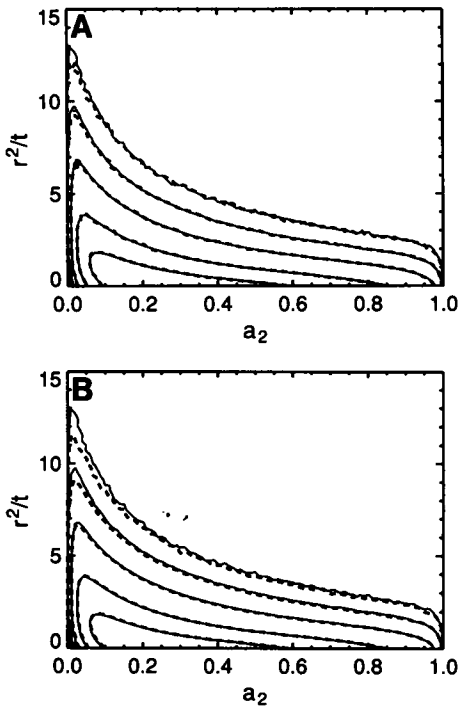

FIGURE 9 Joint distributions of eigenvalue ratio a_2 and displacement r^2/t for a pure random walk on a continuum, for 10^8 trajectories. These are normalized so that the total volume is one. Contour values are 5×10^{-7}, 5×10^{-6}, 5×10^{-5}, 5×10^{-4}, and 2×10^{-3}. Bin sizes are $\Delta r^2/t = 0.25$ and $\Delta a_2 = 0.01$. (*a*) Comparison of continuum (solid lines) and lattice (dashed lines) results for $t = 256$. (*b*) Comparison of continuum results for $t = 256$ (solid lines) and $t = 64$ (dashed lines). The maximum values agree well: 0.004846 for the continuum at $t = 256$, 0.004910 for the lattice at $t = 256$, and 0.004796 for the continuum at $t = 64$. A bin-by-bin comparison of the original histograms shows they agree to 4% or better.

hazardous. It is necessary to set up an algorithm to subdivide the trajectory, and test the algorithm on models like those discussed here, particularly the pure random walk. Work in progress attempts to do this by subdividing a trajectory into segments of all lengths and all starting points. Then each segment is characterized by the parameters already discussed, and the segments not likely to be random walks are identified. Averaging is done only within each segment, so information about the bound-free equilibrium is retained.

Supplemental material will be found on the Biophysics Internet Server. For instructions, see Biophysics on the Internet on the last page of this issue.

I thank K. Jacobson, R. Simson, and A. Kusumi for helpful discussions; the reviewers for helpful comments; and R. Simson for testing some of these methods on his experimental data. This work was supported by National Institutes of Health grant GM38133.

REFERENCES

Anderson, C. M., G. N. Georgiou, I. E. G. Morrison, G. V. W. Stevenson, and R. J. Cherry. 1992. Tracking of cell surface receptors by fluorescence digital imaging microscopy using a charge-coupled device camera. Low-density lipoprotein and influenza virus receptor mobility at 4°C. *J. Cell Sci.* 101:415–425.

de Brabander, M., R. Nuydens, A. Ishihara, B. Holifield, K. Jacobson, and H. Geerts. 1991. Lateral diffusion and retrograde movements of individual cell surface components on single motile cells observed with Nanovid microscopy. *J. Cell Biol.* 112:111–124.

Edidin, M., S. C. Kuo, and M. P. Sheetz. 1991. Lateral movements of membrane glycoproteins restricted by dynamic cytoplasmic barriers. *Science.* 254:1379–1382.

Family, F., T. Vicsek, and P. Meakin. 1985. Are random fractal clusters isotropic? *Phys. Rev. Lett.* 55:641–644.

Fein, M., J. Unkeless, F. Y. S. Chuang, M. Sassaroli, R. da Costa, H. Väänänen, and J. Eisinger. 1993. Lateral mobility of lipid analogues and GPI-anchored proteins in supported bilayers determined by fluorescent bead tracking. *J. Membr. Biol.* 135:83–92.

Foley, J. D., A. van Dam, S. K. Feiner, and J. F. Hughes, 1990. Computer Graphics: Principles and Practice. 2nd ed. Addison-Wesley, Reading, Massachusetts. 504–505.

Ghosh, R. N. 1991. Mobility and clustering of individual low-density lipoprotein receptor molecules on the surface of human skin fibroblasts. Ph.D. thesis, Cornell University, Ithaca, New York. 260 pp.

Ghosh, R. N., and W. W. Webb. 1987. Low density lipoprotein (LDL) receptor dynamics on cell surfaces. *Biophys. J.* 51:A520.

Ghosh, R. N., and W. W. Webb. 1994. Automated detection and tracking of individual and clustered cell surface low density lipoprotein receptor molecules. *Biophys. J.* 66:1301–1318.

Kucik, D. F., E. L. Elson, and M. P. Sheetz. 1990. Cell migration does not produce membrane flow. *J. Cell Biol.* 111:1617–1622.

Kusumi, A., Y. Sako, and M. Yamamoto, 1993. Confined lateral diffusion of membrane receptors as studied by single particle tracking (Nanovid microscopy). Effects of calcium-induced differentiation in cultured epithelial cells. *Biophys. J.* 65:2021–2040.

Lee, G. M., F. Zhang, A. Ishihara, C. L. McNeil, and K. A. Jacobson. 1993. Unconfined lateral diffusion and an estimate of pericellular matrix viscosity revealed by measuring the mobility of gold-tagged lipids. *J. Cell Biol.* 120:25–35.

Popov, S., A. Brown, and M.-m. Poo. 1993. Forward plasma membrane flow in growing nerve processes. *Science.* 259:244–246.

Qian, H., M. P. Sheetz, and E. L. Elson. 1991. Single particle tracking. Analysis of diffusion and flow in two-dimensional systems. *Biophys. J.* 60:910–921.

Quandt, S., and A. P. Young. 1987. The shape of two-dimensional percolation and Ising clusters. *J. Phys. A.* 20:L851–L856.

Rudnick, J., and G. Gaspari. 1987. The shapes of random walks. *Science.* 237:384–389.

Saxton, M. J. 1993. Lateral diffusion in an archipelago: single-particle diffusion. *Biophys. J.* 64:1766–1780.

Sheetz, M. P. 1993. Glycoprotein motility and dynamic domains in fluid plasma membranes. *Annu. Rev. Biophys. Biomol. Struct.* 22:417–431.

Sheetz, M. P., and E. L. Elson. 1993. Measurement of membrane glycoprotein movement by single-particle tracking. *In* Optical Microscopy: Emerging Methods and Applications. B. Herman and J. J. Lemasters, editors. Academic Press, San Diego. 285–294.

Sheetz, M. P., S. Turney, H. Qian, and E. L. Elson. 1989. Nanometre-level analysis demonstrates that lipid flow does not drive membrane glycoprotein movements. *Nature.* 340:284–288.

Šolc, K., and W. H. Stockmayer. 1971. Shape of a random-flight chain. *J. Chem. Phys.* 54:2756–2757.

Zhang, F., G. M. Lee, and K. Jacobson. 1993. Protein lateral mobility as a reflection of membrane microstructure. *BioEssays.* 15:579–588.